Received: 8 January 2021 | Revised: 10 May 2021 | Accepted: 31 May 2021

DOI: 10.1111/jfpp.15702

ORIGINAL ARTICLE

Journal of Food Processing and Preservation | Institute of Food Science + Technology ifst | WILEY

Refractance window (RW) concentration of milk-Part II: Computer vision approach for optimizing microbial and sensory qualities

Asaad R. Al-Hilphy[1] | Haider I. Ali[1] | Sajedah A. Al-IEssa[1] | José M. Lorenzo[2,3] | Francisco J. Barba[4] | Mohsen Gavahian[5]

[1]Department of Food Science, College of Agriculture, University of Basrah, Basrah, Iraq

[2]Centro Tecnológico de la Carne de Galicia, San Cibrao das Viñas, Spain

[3]Área de Tecnología de los Alimentos, Facultad de Ciencias de Ourense, Universidad de Vigo, Ourense, Spain

[4]Preventive Medicine and Public Health, Food Science, Toxicology and Forensic Medicine Department, Nutrition and Food Science Area, Universitat de València, València, Spain

[5]Department of Food Science, National Pingtung University of Science and Technology, Pingtung, Taiwan, ROC

Correspondence
Mohsen Gavahian, Department of Food Science, College of Agriculture, National Pingtung University of Science and Technology, 1, Shuefu Road, Neipu, Pingtung 91201, Taiwan, ROC.
Email: mohsengavahian@yahoo.com

Abstract

This study is the second part of ongoing research on developing a refractive window (RW) milk concentrator. The response surface methodology-computer vision approach provided a platform to maximize process productivity, minimize energy consumption, and optimize microbiological, sensory, and color parameters. The results were compared with the conventional concentration (CC). Experimental conditions were temperatures at 50, 60, and 70°C and pressures of 0.4, 0.6, and 0.8 bar. According to the results, the RW product had a better sensory and microbiological characteristic than CC. The optimum process conditions in terms of shelf-life and sensory properties were the pressure of 0.45 bar and temperature of 66°C. The productivity of RW was higher than that of CC by 110% (2.3 vs. 1.1 L/h). Besides, RW products got a higher score on sensory assessment in comparison with CC. Furthermore, RW significantly increased the shelf-life and decreased the peroxide value of concentrated milk. Results suggested that RW has the potential to be implemented in dairy industry in the future.

Novelty impact statement: The response surface methodology-computer vision approach was found to be a useful platform for process optimization based on sensory and microbiological qualities; The pressure and temperature of 0.45 bar and 66°C were optimal process conditions; refractive window improved the productivity, sensory scores, and reduced the peroxide value in comparison with the conventional method.

1 | INTRODUCTION

Milk is a nutritious material that contains valuable compounds including vitamins, minerals, carbohydrates, fats, proteins, and bioactive peptides (Al-Hilphy et al., 2019). In addition, fresh milk is processed to improve shelf-life and safety or to produce other products. For example, various evaporative operations are employed in the industry to concentrate the milk either to enhance the shelf-life of the product (e.g., condensed milk production) or to prepare a suitable feed for further processes (e.g., production of milk powder and some type of cheese). On the other hand, color is an important consideration in the operation of concentration units and affects product acceptance (Faion et al., 2019; Fernández-Vázquez et al., 2018).

Conventional approaches of concentration have negative effects on milk color. Researchers apply the new technologies in concentrating the milk to obtain a high-quality product (Faion et al., 2019; Moejes et al., 2020; Parmar et al., 2018). Refractance Window (RW) is a novel food-processing technology, which is used for producing products with high quality, and it is utilized in food dehydration at the factories and laboratories (Bernaert et al., 2019; Raghavi et al., 2018). RW works via heating the circulated water which makes it emit infrared radiation, then the part of irradiated energy is

 © 2021 Wiley Periodicals LLC.

transferred via Mylar transparent polyester film (as a window) to the thin layer of liquid food to heat it. Also, the conduction heat transfer takes place between window and food. Another part of energy reflects the water (Abonyiet al., 2002; Zotarelli et al., 2015). There is limited information on the application of this technique to concentrate milk.

Besides, advanced color measurement systems can be interesting for the industry. L^* (luminosity), a^* (redness/greenness), and b^* (yellowness/blueness) are widely accepted parameters for color evaluation that are proposed by the Commission International d'Eclairage. In this regard, the possibility of using computer vision systems (CVS) to measure these color parameters has recently attracted the attention of researchers (Hadimani & Mittal, 2019; Minz & Saini, 2019; Tomasević et al., 2019). Also the applications of CVS, such as digital image processing, in combination with mathematical models for the determination of other food properties (e.g., fat content and viscosity) can be considered as a future technology in the food processing industry, considering the potential benefits and recent progress in this area of the research (Lei & Sun, 2019; Taheri-Garavand et al., 2019). The current study aims to investigate the possibility of milk concentration by RW technology and to understand the effects of temperature and pressure of RW process on some physical properties of the product such as browning index (BI).

Besides, an online CVS-mathematical approach was developed to predict some quality parameters (e.g., fat content, viscosity, and pH) of the RW concentrated milk. The fitting of the proposed method was verified by comparing the experimental data and predicted data. In our previous study (Al-Hilphy et al., 2020), a new RW apparatus was designed for milk concentration, and its performance on some physicochemical characteristics of the milk was evaluated.

In the present study, the previously developed system and information were used to assess the influence of the RW on the organoleptic and microbiological properties of the concentrated milk. These include qualitative attributes (e.g., color parameters and browning index), the mass of water removed from milk, productivity with optimization of parameters, microorganisms' inactivation, acidity, peroxide value during the storage periods as well as sensory evaluation. The authors believed that these parameters are very important to evaluate RW-concentrated milk, which can help with the future possible commercial application of this emerging processing technology.

2 | MATERIALS AND METHODS

2.1 | Fresh milk

Fresh bovine milk was provided from the station of Agriculture research, University of Basrah. The milk was preserved at a temperature of 5℃. A water bath (GFL 1,008, German) was used to heat the raw milk (4.721 kg, 4.11% fat, 13.1% TSS) to 40℃ then 88 g of milk powder (Alsabah, Iran, 0.2% fat, 95% TSS) and 191 g of dairy cream (Barmezan, Iran 30% fat) were added to the raw milk to produce standardized milk (5 kg, 5.01% fat, 15.7% TSS). After that, concentration processes were performed using RW and conventional methods.

2.2 | Concentration of milk

RW concentrator manufactured by Al-Hilphy et al. (2020) was used to concentrate milk. The schematic diagram of RW concentrator operation is illustrated in Figure 1. It consists of a concentration unit made of Pyrex, a heating unit, and a control unit. Briefly, 5 L of the standardized milk was placed in the RW concentrator and the temperature was raised to 95℃. The experiments were carried out using partial vacuums at pressure values of 0.4 to 0.8 bar and temperature values of 50 to 70℃. The desired concentration was at 26% TSS.

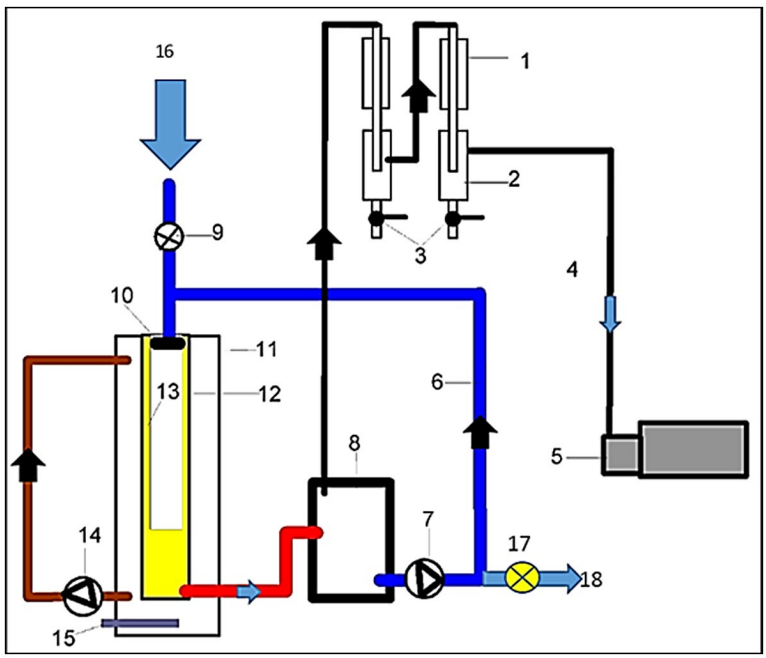

FIGURE 1 Operation layout of the Refractance window milk concentrator. 1: heat exchanger; 2: steam hunter; 3: valves; 4: pipe; 5: vacuum pump; 6: milk pipe; 7: milk pump; 8: vacuum container; 9: valve; 10: milk distributor; 11: hot water tank; 12: Pyrex cylinder; 13: milk layer; 14: hot water pump; 15: heater; 16: raw milk input; 17: valve; 18: milk outlet

In conventional concentration (CC) (Figure 2), 5 L of standardized milk was placed in a pan made of stainless steel provided with a double jacket and the space filled with water. Water was heated using a 2-kW power electric heater (Orbon, India). Milk was concentrated to 26% TSS by heat transfer from heated water to milk via the wall of pan. A digital gauge controller (LTR5/LEA Electronic, Italy) was used to monitor milk temperature. All experiments were executed by triplicates.

2.3 | Color assessment

The CVS in the current study consists of a computer, 4 LED lamps (LB13W, Konnice Co., China), and an HD camera (IP67 Endoscope, Mileseey, China), as illustrated in Figure 3. The color of raw and concentrated milk was determined using image processing. In this regard, the Image J program (National Institutes of Health, United States) has been used to measure values of L^*, a^*, b^*. The color parameters were converted to standard values as shown in Equations 1–3 according to (Wasnik et al., 2019; Yam & Papadakis, 2004):

$$L^* = \frac{L}{255} \times 100 \tag{1}$$

$$a^* = \frac{240a}{255} - 120 \tag{2}$$

$$b^* = \frac{240b}{255} - 120 \tag{3}$$

where L_o^*, a_o^*, and b_o^* are the, luminous, redness-greenness, yellowness-blueness of raw milk (also calculated using Equations 1–3) and L^*, a^*, and b^* for the concentrating milk.

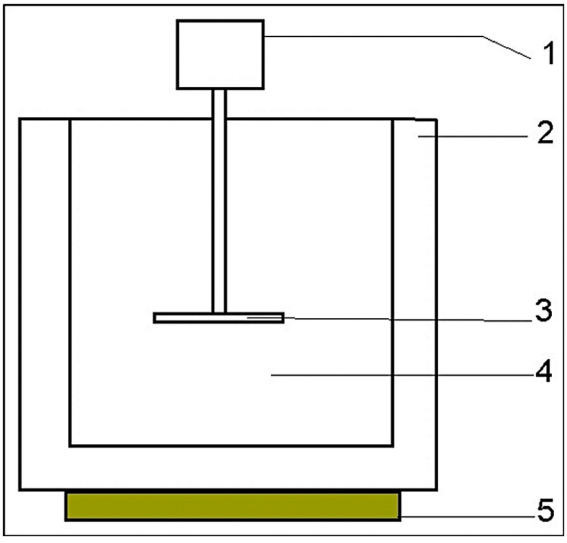

FIGURE 2 The schematic presentation of the conventional milk concentration system: 1: motor; 2: jacket filled with water; 3: impeller, milk; 5: electrical heater

Also, the color density (Chroma) and Hue angle (h) are given in Equations 4 and 5, (Wasnik et al., 2019; Yam & Papadakis, 2004):

$$\Delta C = \sqrt{\left(a_o^* - a^*\right)^2 + \left(b_o^* - b^*\right)^2} \tag{4}$$

$$h = \tan^{-1}\left(\frac{b^*}{a^*}\right) \tag{5}$$

where ΔC is the Chroma, h is the hue angle (rad).

The BI was calculated according to Equations 6 and 7 to evaluate the effects of the concentration process on the degree of brown color development and is given in Equations 6 and 7 (Palou et al., 1999):

$$\mathrm{BI} = \frac{\left[100\left(X - 0.31\right)\right]}{0.172} \tag{6}$$

$$X = \frac{\left(a^* + 1.75L^*\right)}{\left(5.645L^* + a^* - 3.1012b^*\right)} \tag{7}$$

where BI is the Browning Index, a^* is the redness-greenness, L^* is the luminous value, and b^* is the yellowness-blueness of samples.

2.4 | Productivity and thermo-physical properties

The productivity is given in Equation 8 as follows:

$$\mathrm{Prod.} = \frac{V_m}{t} \tag{8}$$

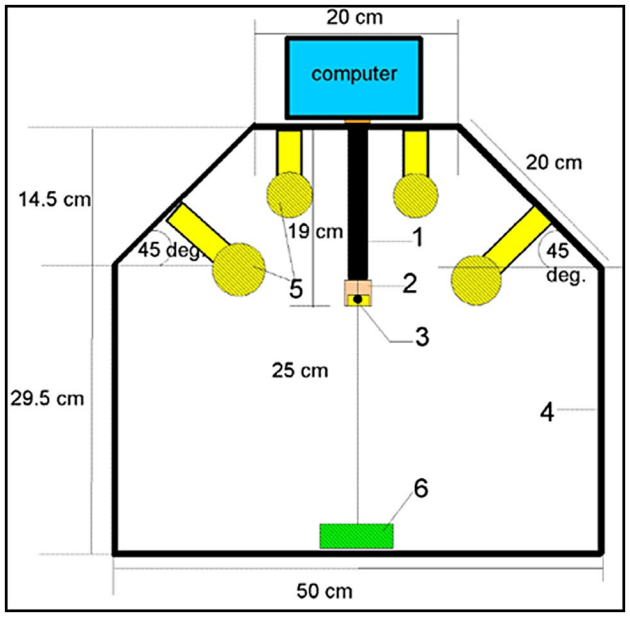

FIGURE 3 The image acquisition system used in the present study: A: a schematic representation and the system components (1: plastic pipe; 2: camera cover; 3: camera; 4: wood box; 5: LED lamps; 6: sample)

where V_m is the volume of concentrated milk (L), t is the total concentration time (h), "prod." is the productivity of concentrated milk (L/h).

Total heating energy was calculated from Equation 9 (Darvishi et al., 2015):

$$Q = M_m C_p \left(T_f - T_i\right) + M_w L_h \tag{9}$$

where Q is the total heating energy used for heating the milk (kJ), M_m is the milk mass (kg), C_p is the specific heat (kJ/kg ℃), T_f is the final milk temperature (℃), T_i is the initial milk temperature (℃). M_w and L_h are the mass of evaporated water (kg) and the latent heat of vaporization of water (kJ/kg), respectively.

2.5 | Mass of evaporated water

Mass of evaporated water is given in Equation 10:

$$M_w = mp_{\text{in}} \left[1 - \frac{\text{TSS}_{\text{in}}}{\text{TSS}_{\text{out}}}\right] \times t \tag{10}$$

where TSS_{out} is the outlet of concentrated milk, TSS_{in} is the inlet of standardized milk, mp_{in} is the mass flow rate of milk (kg/s), and t is the total time (s).

2.6 | LMTD

LMTD is given by Equation 11 (Silveira et al., 2013):

$$\text{LMTD} = \frac{\left(T_\theta - T_\mu\right) - \left(T_\tau - T_\delta\right)}{\ln\left[\frac{T_\theta - T_\mu}{T_\tau - T_\delta}\right]} \tag{11}$$

where T_θ is the cold water temperature (℃), T_τ is the hot water temperature, T_μ is the cold milk temperature (℃), T_δ is the hot milk temperature (℃), and LMTD is the logarithm mean temperature differences (℃).

2.7 | Titratable acidity

Titratable acidity was achieved according to the (A.O.A.C., 2016), by taking 10 ml of raw milk samples and concentrated milk, then adding it into a beaker. Three drops of phenolphthalein reagent at a concentration of 1% were added to it, then NaOH 0.1 normality was added by stirring until the pink color appeared. The percentage of acidity was calculated based on the lactic acid from Equation 12:

$$\text{Acidity}\,(\%) = \frac{\text{NaOH volume} \times N \times 0.09}{V} \tag{12}$$

where N is the normality in the sample weight (ml).

2.8 | Microbiological tests

Microbiological tests were executed on RM, CC, and RW samples at days 0, 30, 60, and 90 of refrigeration. Microbiological tests were executed according to a protocol described in the literature (Keyser et al., 2008). Briefly, under sterile conditions, 11 ml of milk sample was added to 99 ml of peptone water, which contains 0.1% peptone. The sample was mixed well, and then the decimal dilutes were prepared to estimate the total count of bacteria, psychrophiles, coliforms, *Staphylococcus aureus*, yeasts, lipolytic bacteria, and proteolytic bacteria. For the proteolytic and lipolytic bacteria counts, the method mentioned by Harrigan and Mccance (1976) was followed.

2.9 | Detection of the presence of the alkaline phosphatase

The enzymatic method mentioned by Belfield and Goldberg (1971) to detect the presence of the alkaline phosphatase in raw and concentrated milk samples using the commercial kit was provided by Egyptian Company Biotechnology.

2.10 | Peroxide number

The method mentioned in A.O.A.C. (2016) was followed to estimate the peroxide number of milk samples. A 5 ± 0.05 g of the milk sample was weighed and placed in a conical flask, and 30 ml of a mixture consisting of chloroform and ice acetic acid was added at a ratio of 3:2 volume and shaken in a circular motion to dissolve the samples. A solution of saturated potassium iodide (5 ml) was added, and continued to shake for a minute, and it was stored for 30 min in a dark place. Then 30 ml of distilled water was added to wash the iodine, followed by 3–5 drops of a guide solution, 1% starch, and the mixture was crushed with 0.01 g of sodium thiosulfate until the blue color disappeared. About 5 ml of distilled water was used to prepare a Blank solution instead of the milk sample by following the same previous steps. Peroxide number is given in Equation (13):

$$\text{PN} = \frac{A \times N}{W} \times 1000 \tag{13}$$

where PN is the peroxide number, A is sodium thiosulfate (mm), N is the normality, and W is the sample weight (g).

2.11 | Sensory assessment

The sensory evaluation was performed according to Clark et al. (2009). Ten trained panelists from the Department of Food Science, University of Basrah, Iraq, to assess concentrated milk by RW and CC via odors (40%), consistency and texture (30%), color (10%), taste (10%) and overall acceptability (10%). The training of panelists

included the assessment of various milk samples to describe and quantify odors, consistency, texture, color, taste, and overall acceptability attributes using descriptive terms and scale values of odors (40%), consistency and texture (30%), color (10%), taste (10%), and overall acceptability (10%). This procedure was repeated until a reasonable degree panel consensus was accomplished.

2.12 | Experimental design and statistical analysis

The preliminary experiments were executed to choose the range of independent variables (temperature 50, 60, and 70°C; pressure of 0.4, 0.6, and 0.8 bar) as given in Table 1. Moreover, temperature and pressure were optimized using RSM using the central composite design (CCD). Design Expert Software ver. 7 (Stat-Ease Inc., United States) was used. The independent variables were coded as +1, 0, and −1, which represented the highest, medium, and lowest values, respectively. To predict the dependent variables (L^*, b^*, a^*, h, ΔC, IB, total heating energy, LMTD, productivity, and mass of evaporated water), the second order polynomial model was used according to Equation 14 (Khuri & Cornell, 2019):

$$Y_i = \alpha_0 + \alpha_1 P + \alpha_2 T + \alpha_{12} PT + \alpha_{11} P^2 + \alpha_{22} T^2 \quad (14)$$

where Y is the responses (L^*, a^*, b^*, h, ΔC, total heating energy, LMTD, productivity, and mass of evaporated water), P is the pressure; α_0, α_1, α_2, α_{12}, α_{11}, α_{22} are regression coefficients of constant; linear of P, T, and PT (interaction terms), quadratic of P^2, and T^2, respectively.

Numerical methods were used to optimize milk concentration conditions (0.4, 0.6, and 0.8 bar pressure, and 50, 60, and 70°C temperature) to produce concentrated milk with good color properties, that is similar to those described in the published papers (McDermott et al., 2016; Misawa et al., 2016; Scarso et al., 2017). In this regard, the minimum values of b^*, a^*, h, and IB, as well as the maximum values of L^* and ΔC were optimized using Design Expert software at different conditions of pressure and temperature.

For statistical analysis, The Design Expert software was used to statistical analyze data. To assess the differences among means, analysis of variance has been used at p-value level of .05 to assess parameters of the second-order models. All experiments were repeated three times. The results of the current study were mean ± standard deviation.

3 | RESULTS AND DISCUSSION

3.1 | Temperature profile

Figure 4 illustrated the heating curve of milk during RW and CC. In the RW process, the milk temperature was increased from 40 to 95°C during the first 10 min, followed by a 10 min of holding time. According to the results, the time required to reach 95°C was 11 and 160 min for RW and CC, respectively. This indicates a substantial reduction in the come-up time of the process using the innovative RW technique. RW reduced the come-up time because of a better heat transfer rate in a thin layer of milk on the heated Pyrex glass wall compared with that of CC where milk samples were placed in a container. In the RW process proposed in the present study, the concentrated milk was immediately cooled to 50–70°C by applying a vacuum of 0.4–0.8 bar and reducing the temperature of heat exchange medium (water) to 20°C. Besides, the total time required to concentrate milk was 60 and 265 min, for RW and CC process, respectively. This indicated that replacement of CC with RW can save a substancial amount of the time required to concentrate the same amount of milk. In other world, RW required about 23% of processing time in comparison with CC.

TABLE 1 Central composite design matrix for the effect of pressure and temperature on the dependent variables (Productivity, Heating energy) of the milk concentrated by the Refractance window

Run	Pressure (bar)	Temperature (°C)	Productivity (L/h)	Total heating energy (kJ)	Mass of evaporated water (kg)	LMTD (°C)
1	0.40	50	2.58 ± 0.140	1.24 ± 0.001	1.88 ± 0.131	10.80 ± 0.011
2	0.80	50	0.75 ± 0.110	0.69 ± 0.011	0.76 ± 0. 202	10.82 ± 0.021
3	0.80	60	0.72 ± 0.211	0.87 ± 0.023	0.83 ± 0.100	14.07 ± 0.012
4	0.80	70	0.88 ± 0.362	0.99 ± 0.052	0.79 ± 0.205	16.83 ± 0.045
5	0.60	60	1.37 ± 0.050	0.93 ± 0.032	1.13 ± 0.140	13.79 ± 0.033
6	0.40	70	3 ± 0.1330	1.44 ± 0.060	2.00 ± 0.230	16.83 ± 0.020
7	0.40	60	2.61 ± 0.911	1.34 ± 0.021	1.94 ± 0.141	13.85 ± 0.062
8	0.60	60	1.33 ± 0.160	0.95 ± 0.010	1.15 ± 0.211	13.80 ± 0.042
9	0.60	60	1.24 ± 0.172	0.98 ± 0.030	1.20 ± 0.222	13.83 ± 0.062
10	0.60	60	1.3 ± 0.210	0.98 ± 0.080	1.20 ± 0.190	14.00 ± 0.032
11	0.60	70	1.28 ± 0.070	1.10 ± 0.044	1.25 ± 0.203	16.83 ± 0.051
12	0.60	50	1.32 ± 0.621	0.79 ± 0.090	1.06 ± 0.210	10.72 ± 0.062
13	0.60	60	1.25 ± 0.193	0.98 ± 0.003	1.20 ± 0.112	13.95 ± 0.090

Abbreviation: LMTD, logarithmic mean temperature difference.

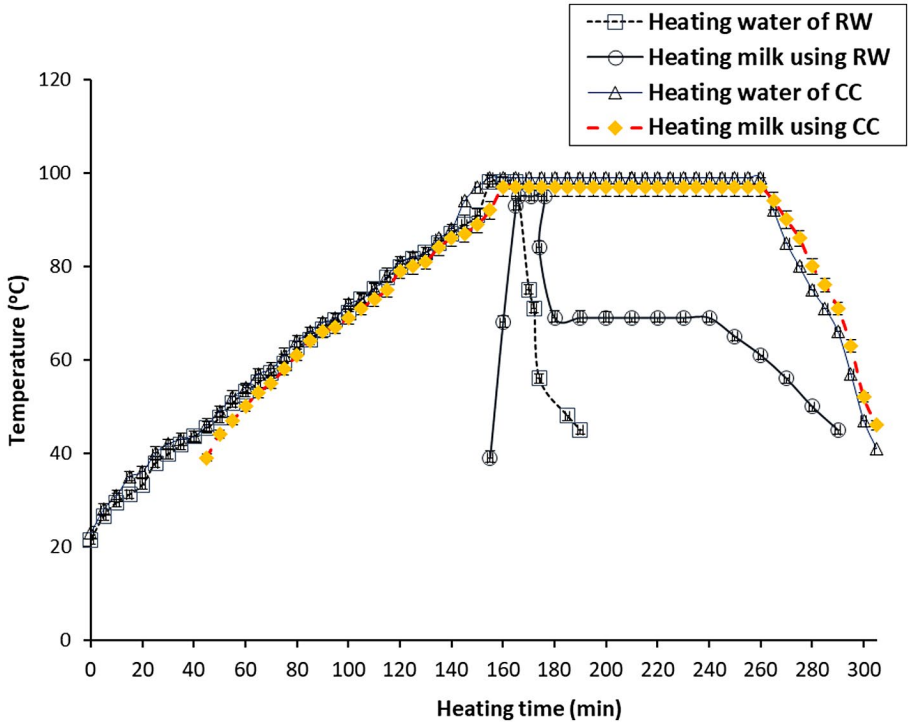

FIGURE 4 Temperature profile of milk and water samples. CC, conventional concentration; RW, refractance windows

3.2 | Productivity and thermo-physical properties

3.2.1 | Productivity

Table 1 presented a matrix of CCD for the temperature (°C) and pressure (bar) and on the productivity of concentrated milk by RW. The productivity of the concentrated milk using RW ranged between 3 L/h at 0.60 bar pressure and 80°C temperature and 0.72 L/h using a pressure of 0.80 bar and a temperature of 60°C. In addition, productivity raised significantly ($p < .05$) as temperature and pressure increased. This is due to the increase of the vacuum pressure, which decreased the boiling point and increased the evaporation rate.

Table 2 indicated that the mathematical model, pressure, and squared pressure have a significant effect ($p < .05$) on productivity. By contrast, there is no significant effect of Lack of Fit. The statistical parameters for R-Squared was 0.9904, Adj R-Squared was 0.9835, Pred R-Squared was 0.9254, Adeq Precision was 33.785, and Std. Dev. was 0.095, and these parameters showed that the RCM can be used for predicting productivity, as given in Equation 15:

$$\text{Prod.} = +8.66622 - 15.58371P - 0.050005T - 0.036866PT + 10.77469P^2 + 6.7016810^{-4}T^2 \quad (15)$$

Figure 5 drawn by the RSM for pressure and temperature. At a temperature of 50°C and a pressure of 0.40 bar, the productivity of concentrated milk by RW was 2.59 L/h and decreased to 0.79 L/h using a 0.80 bar pressure and 50°C temperature. Moreover, productivity reached 3 L/h using 0.40 bar pressure and 70°C temperature. This observation might be due to an increase in the amount of evaporated water with reducing the pressure and increasing temperature (Morison et al., 2006).

3.2.2 | Total heating energy

Table 1 shows the matrix of the CCD for the influence of both temperature and pressure on the energy (Q) needed to heat the concentrated milk by the RW. The results indicated that the Q values ranged from 0.69 kJ at pressure of 0.80 bar and 50°C to 1.44 kJ at 0.40 bar pressure and 70°C temperature. This is due to the high temperature that increases the sensible heat, where the difference in the temperatures between the surrounding and the processed milk increased (Silveira et al., 2015; Tanguy et al., 2019).

Table 2 disclosed that there was a significant effect ($p < .05$) for the mathematical model and the independent variables, the squared pressure, the overlap between them did not show a significant effect of the temperature squared, in addition to that, the statistical analyses showed no significant ($p > .05$) effect of Lack of Fit. R-Squared was 0.9936, adjusted R-Squared was 0.9890, adequate Precision was 50.412, and Std. Dev. was 0.022. These depicted that the nonlinear multimathematical model can be used to predict the energy required for heating:

$$Q = +2.14685 - 6.35328P + 0.022735T + 0.014442PT + 3.55594P^2 - 1.48913\times10^{-4}T^2 \quad (16)$$

As for the interfere between the independent variables, as clarified in 3D Figure 5b drawn by the RSM, the value of Q was 1.227 kJ

TABLE 2 ANOVA for response surface quadratic and reduced quadratic models for independent variables (color components)

	Productivity (L/h)		Total heating energy (kJ)		Mass of evaporated water (kg)		LMTD	
Source	SS	*p*-value	SS	*p*-value	SS	*p*-value	SS	*p*-value
Model	6.430	<.0001	0.531	<.0001	2.120	<.0001	54.981	<.0001
P	5.680	<.0001	0.360	<.0001	1.971	<.0001	9.473E-003	.309
T	0.041	.0687	0.113	<.0001	0.019	.010	54.930	<.0001
$P \times T$	0.022	.1628	3.337E-003	.035	1.992E-003	.290	1.021E-004	.912
P^2	0.511	.0001	0.056	<.0001	0.120	<.0001	0.012	.252
T^2	0.012	.2773	6.125E-004	.300	1.637E-003	.334	0.039	.062
Residual	0.063	–	3.433E-003	–	0.011	–	0.055	–
Lack of fit	0.050	.0688	1.746E-003	.370	6.145E-003	.284	0.018	.616
Pure error	0.012	–	1.687E-003	–	4.510E-003	–	0.037	–
Cor total	6.490	–	0.530	–	2.130	–	55.030	–
Std. Dev.	0.095	–	0.022	–	0.039	–	0.089	–
R^2	0.990	–	0.993	–	0.995	–	0.999	–
Adj R^2	0.983	–	0.989	–	0.991	–	0.998	–
Adeq precision	168.280	–	50.412	–	47.409	–	101.981	–

Abbreviations: LMTD, logarithm mean temperature differences; SS, sum of squares.

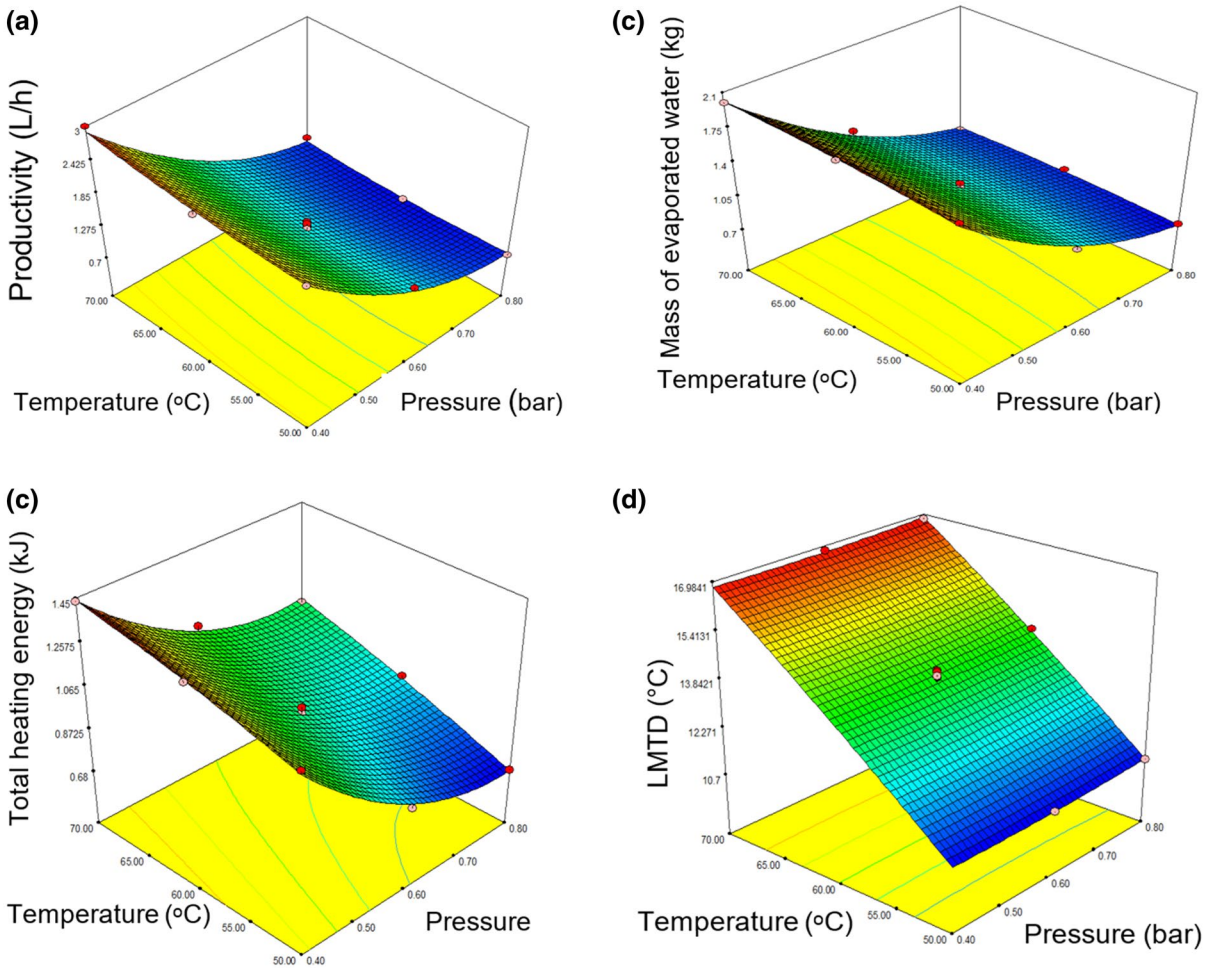

FIGURE 5 Response surface plot of (a): productivity, (b): total energy, (c): mass of evaporated water, (d): LMTD, as a function of process temperature and pressure

when using 0.40 bar pressure and a temperature of 50°C, and decreased to 0.682 kJ at 0.80 bar pressure and temperature of 50°C. The value of *Q* decreased from 1.44 kJ at 0.40 bar pressure and 70°C temperature to 1.01 kJ at a pressure of 0.80 bar and 70°C temperature. We concluded from this that the value of *Q* is affected by the interference as it increases with increasing temperature and decreasing pressure (Pehlivan & Özdemir, 2012).

3.2.3 | The mass of evaporated water

Table 1 presents the matrix of the CCD for the influence of both temperature and pressure on the mass of evaporated water from the concentrated milk using RW. The results indicated that the values of the mass of the evaporated water ranged between 0.76 kg at a pressure of 0.80 bar and a temperature of 50°C and 2.00 kg at a pressure of 0.40 bar and a temperature of 70°C. Here, vacuum pressure and high temperature had significant effects in increasing the amount of evaporated water. An increase in temperature increases the rate of evaporation, as well as decreasing pressure led to an increase in moisture withdrawal. The evaporation rate depends on the operating conditions such as the heat distribution system, and the product properties such as surface tension and viscosity (Paramalingam et al., 2000; Pehlivan & Özdemir, 2012).

Table 2 disclosed that the mathematical model, the two independent factors, and the squared pressure had significant effects ($p < .05$). By contrast, there is no significant effect for the interference and the squared temperature on the mass of evaporated water. The statistical parameters illustrated that R-Squared was 0.9950, Adjusted R-Squared was 0.9914, adequate Precision was 47.409, and Std. Dev. was 0.039. These statistical indicators disclosed that it is possible to adopt the nonlinear equation with multiple correlations in predicting the mass of evaporated water:

$$M = +3.15221 - 8.42483P + 0.041474T - 0.011159PT + 5.19264P^2 - 2.43455 \times 10^{-4}T^2 \quad (17)$$

The overlap between independent variables as clarified in the 3D Figure 5c drawn by the RSM, the mass of evaporated water was 1.85 kg using 0.4 bar pressure and a temperature of 50°C, and it decreased to 0.75 kg at pressure of 0.8 bar and 50°C temperature, and it reached 2.01 kg when the pressure reached 0.4 bar and temperature was 70°C. Mass of evaporated water was decreased to 0.82 kg at 0.8 bar and 70°C. This is due to the reduction of pressure which results in an increase in the amount of evaporated water (Silveira et al., 2013). da Silva et al. (2014) showed that the latent heat of water vaporization increases with increasing temperature.

3.2.4 | LMTD

Table 1 presents the matrix of the CCD for the impact of independent variables on the LMTD (°C) of concentrated milk by RW. The results revealed that the minimum LMTD value was 10.80°C at 0.40 bar pressure and 50°C temperature, and the maximum value reached 16.83°C at a pressure of 0.60 bar and a temperature of 70°C. This was due to the increase in milk temperature. Yanniotis (2007) showed that the difference in total temperature in the multi-effect evaporator increased with an increase in pressure in the last effect, which enhanced the final product concentration. Moreover, direct variation in the temperatures of the heat transfer medium allows the transfer of solutes to improve the quality of the processed food (Konovalov et al., 2004).

The ANOVA in Table 2 shows that there was a significant ($p < .05$) influence for the mathematical model and temperature, while pressure, factors squares, and interactions were not significant ($p > .05$). In addition, the Lack of Fit was insignificant. R-Squared was 0.9990, Adjusted R-Squared was 0.9983, Adequate Precision was 101.981 and Std. Dev. was 0.089. Statistical parameters disclosed that the mathematical model can be used to predict LMTD as given in Equation 18:

$$\text{LMTD} = -8.15297 - 1.64829P + 0.44636T - 2.52660 \times 10^{-3}PT \quad (18)$$

As for the interaction between independent variables, as clarified in the 3D Figure 5d drawn by the RSM. The value of LMTD reached 10.75 m when using 0.4 bar pressure and 50°C temperature, and it raised to 10.84°C at 0.8 bar pressure and 50°C temperature. It is also noted from the three-dimensional figure that the impact of temperature is higher than the impact of pressure, as temperature is a significant factor affecting LMTD at all pressure values.

3.3 | Color parameters of samples as affected by concentration processes

3.3.1 | Lightness

Table 3 illustrated that the measured L^* values ranged between 69.22 at 0.8 bar pressure and 50°C temperature and 75.30 at 0.6 bar pressure and 60°C temperature (run 10). According to the results, L^* values were increased as temperature increases, and pressure decreased. This observation indicates that a decrease in pressure (vacuum) can improve the color of concentrated milk. Similar to the present study, Rossi et al. (2018) declared that the L^* the value of milk was 66.7. Another study also reported disclosed that the L^* the value of a milk sample was 81.06 (Ávila et al., 2017).

Table 4 illustrated that the reduced cubic model (RCM) and the interaction between temperature and pressure have a significant effect ($p < .05$) on the L^* value of samples. On the other hand, the temperature, pressure, squared pressure, squared temperature, the overlap between squared pressure and temperature, and interaction between pressure and squared temperature have insignificant impacts on the L^* value, as well as the effect of Lack of Fit was insignificant. The statistical parameters illustrated that R-Squared, adjusted R-Squared, Adequate Precision, and Standard deviation for the RCM of L^* were 0.8877, 0.7304, 8.861, and 0.87, respectively (Table 4).

TABLE 3 Results of color parameters for the concentrated milk using Refractance window measured under different process conditions

Run	*P*	*T*	*L**	*a**	*b**	Δ*C*	*h (rad)*	IB
1	0.40	50	74.80 ± 1.20	−2.59 ± 0.20	8.94 ± 0.29	7.59 ± 0.20	−1.29 ± 0.10	9.72 ± 0.13
2	0.80	50	69.22 ± 1.27	−3.29 ± 0.03	8.71 ± 0.36	5.00 ± 0.30	−1.21 ± 0.03	9.43 ± 0.24
3	0.80	60	75.29 ± 0.90	−0.71 ± 0.04	10.35 ± 0.26	7.54 ± 0.45	1.19 ± 0.04	13.58 ± 0.12
4	0.80	70	75.25 ± 1.33	−4.71 ± 0.01	11.53 ± 0.88	7.6 ± 0.70	−1.18 ± 0.01	11.34 ± 0.83
5	0.60	60	75.29 ± 1.07	−2.59 ± 0.10	8.24 ± 0.65	7.03 ± 0.11	−1.27 ± 0.01	8.63 ± 0.29
6	0.40	70	75.27 ± 2.10	−1.41 ± 0.02	7.06 ± 0.25	9.01 ± 0.28	−1.37 ± 0.05	8.12 ± 0.76
7	0.40	60	75.29 ± 1.70	−3.76 ± 0.22	10.59 ± 0.60	7.54 ± 0.43	−1.23 ± 0.03	10.88 ± 0.77
8	0.60	60	75.25 ± 2.21	−2.59 ± 0.19	8.24 ± 0.67	4.01 ± 0.56	−1.27 ± 0.05	8.63 ± 0.86
9	0.60	60	75.00 ± 2.28	−2.00 ± 0.03	9.30 ± 0.34	6.93 ± 0.23	−1.36 ± 0.03	11.25 ± 0.98
10	0.60	60	75.30 ± 3.01	−2.59 ± 0.13	8.23 ± 0.22	7.00 ± 0.99	−1.27 ± 0.04	8.62 ± 0.99
11	0.60	70	75.29 ± 1.73	−2.82 ± 0.12	8.71 ± 0.65	7.54 ± 0.55	−1.26 ± 0.01	9.08 ± 1.03
12	0.60	50	75.28 ± 0.99	−2.35 ± 0.22	8.24 ± 0.33	7.49 ± 0.23	−1.30 ± 0.01	8.86 ± 0.98
13	0.60	60	75.29	−2.59 ± 0.26	8.24 ± 0.28	6.85 ± 0.46	−1.27 ± 0.02	8.63 ± 0.78

Abbreviations: *a**, redness-greenness; *b**, blueness-yellowness; Δ*C*, color density; h, hue angel (rad); *L**, lightness; *P*, pressure (bar); *T*, temperature (°C).

TABLE 4 ANOVA for response surface quadratic and reduced quadratic models for independent variables (color components)

	*L**		*a**		*b**		Δ*C*		*h*		IB	
Source	SS	*p*-value	SS	*p*-value	SS	*p*-value	SS	*p*-value	SS	*p*-value	SS	*p*-value
Model	30.210	.037	11.17	.005	2.670	.044	18.400	.0007	2.791	.335	20.272	.330
P	4.653E-007	.999	4.682	.001	0.330	.080	3.380	.0013	1.203	.127	3.621	.225
T	2.533E-005	.995	0.110	.368	5.542	.494	0.164	.2158	3.360E-005	.993	0.022	.917
$P \times T$	7.820	.024	1.670	.012	4.741	.021	6.420	.0003	2.936E-003	.934	3.080	.258
P^2	1.180	.269	0.016	.721	1.310	.029	2.121	.0036	1.202	.128	10.170	.068
T^2	1.1912	.267	0.510	.087	4.470	.194	0.056	.4414	0.981	.162	4.971	.166
$P^2 \times T$	3.610	.082	0.042	.571	3.191	–	0.012	.7161	2.821	–	0.001	.982
$P \times T^2$	2.601	.124	8.531	.0003	1.2830	–	8.530	.0001	2.801	–	0.504	.628
Residual	3.820	–	0.573	–	17.870	–	0.402	–	7.150E-003	–	9.465	–
Lack of fit	2.510	.050	0.290	.110	2.673	.138	0.1810	.1453	5.610	<.0001	3.970	.164
Pure error	1.322	–	0.280	–	0.331	–	0.223	–	–	–	5.501	–
Cor total	34.030	–	11.740	–	5.540	–	18.801	–	–	–	29.730	–
Std. Dev.	0.871	–	0.341	–	0.800	–	0.280	–	0.630	–	1.382	–
R^2	0.887	–	0.951	–	0.749	–	0.978	–	0.497	–	0.681	–
Adj R^2	0.730	–	0.883	–	0.570	–	0.949	–	0.138	–	0.236	–
Adeq precision	8.861	–	13.862	–	6.787	–	22.52	–	3.953	–	−14.776	–

Abbreviation: SS, sum of squares.

These statistical parameters indicated that the RCM can be used for predicting *L** value of concentrated milk at various process conditions (pressure and temperature). The RCM is given in Equation 19:

$$L^* = +132.87958 + 22.50961P - 3.17594T + 4.13764PT - 263.01303P^2 + 0.035301T^2 + 4.11109P^2T - 0.069765PT^2 \quad (19)$$

The response surface graph of *L** is presented in Figure 6a. The highest value for *L** was 75.63 at 0.80 bar pressure and 70°C temperature, which decreased to 69.54 when temperature and pressure reached 50°C and 0.80 bar, respectively. Increasing the process pressure reduced the evaporation rate, resulted in a longer process duration, and negatively affected the *L** value. Also, *L** value reached 75.61 when temperature and pressure were 70°C and 0.4 bar, respectively. Besides, *L** value was insignificantly ($p < .05$) increased from 75.13 to 75.61 when

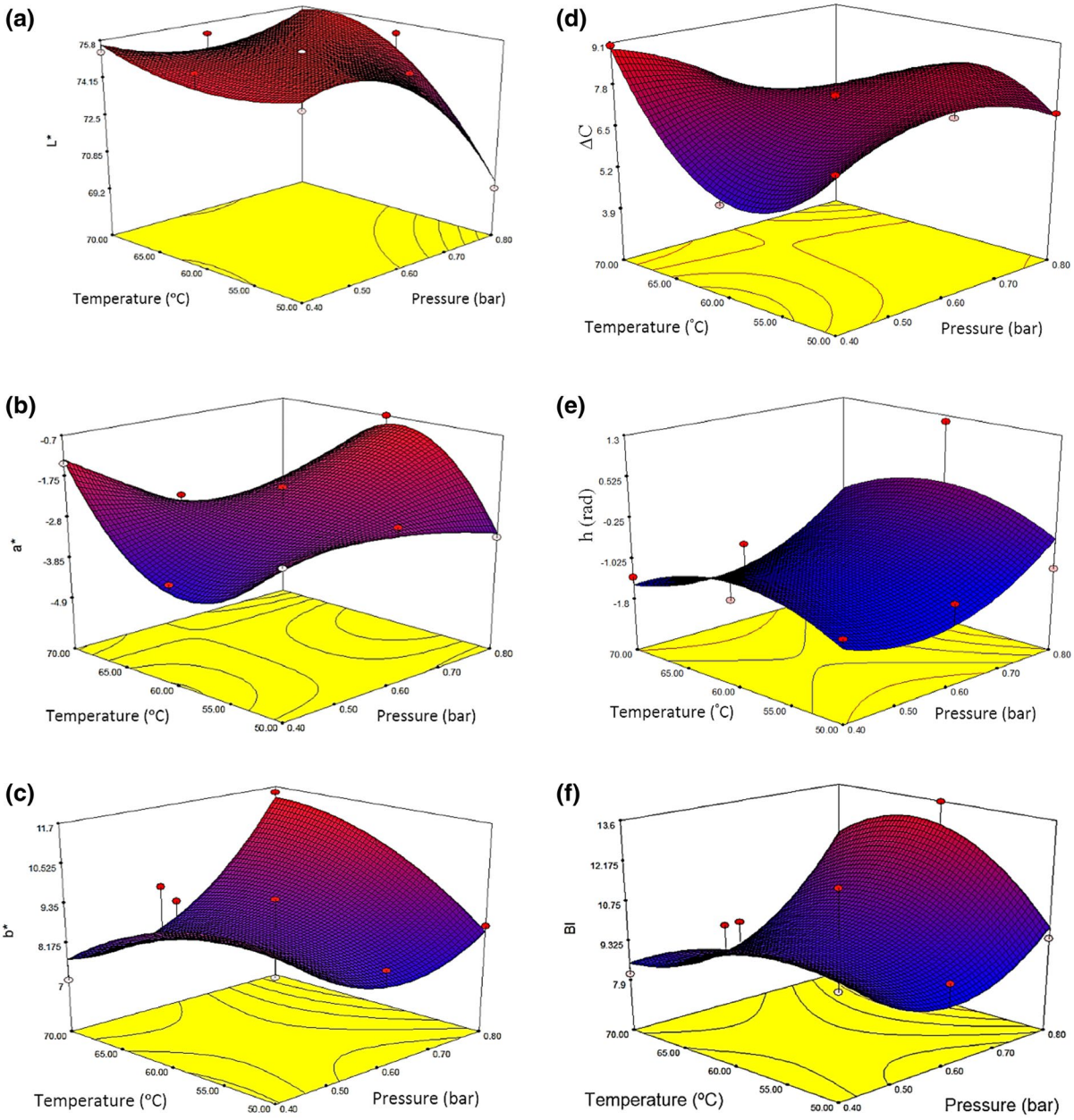

FIGURE 6 Response surface plot of (a): L^* value, (b): a^* value, (c): b^* value, (d): ΔC, and (e): h value, (f): BI as a function of process temperature and pressure

temperature rose from 50 to 70°C at a pressure of 0.4 bar. On the other hand, at a pressure of 0.8 bar, L^* value significantly increased from 69.54 to 75.62 as temperature increased from 50 to 70°C, respectively. Scarso et al. (2017) and Rossi et al. (2018) disclosed that the L^* the value for different milk samples were 81.6 and 66.7, respectively.

3.3.2 | Redness-greenness

The measured a^* values at a pressure of 0.8 bar ranged between −0.71 and −4.71, for temperatures of 60–70°C (Table 3). All a^* values have a negative signal (very small greenness and without redness). Owens et al. (2001) found that L^* and a^* values of milk were 82.1 and −4.06, respectively. The results disagreed with Gaze et al. (2015) who clarified that a^* the value of concentrated milk type *Dulce de Leche* ranged from 13.60 ± 0.02 to 16.90 ± 0.05. The results were agreed with Scarso et al. (2017) who disclosed that a^* the value of milk was −3.88. Finally, Rossi et al. (2018) found that a^* value of milk was 0.25, whereas Ávila et al. (2017) observed a^* value of −1.85.

ANOVA for RCM of a^* is clarified in Table 4. The RCM, pressure, the interaction between temperature and pressure, and the pressure and squared temperature had a significant effect on the a^*. In addition, Lack of Fit was not significant ($p > .05$). Statistics parameters were R-Squared = 0.9516, Adjusted R-Squared = 0.8839, Ad0.80 bar adequate Precision = 13.862, and Standard deviation = 0.34. These indicators showed that the RCM (Equation 20) can be used to predict the redness-greenness (a^*):

$$a* = 230.26077 - 394.13386P - 8.26002T + 14.32203PT - 28.38140P^2 + 0.071579T^2 + 0.44118P^2T - 0.12646PT^2 \quad (20)$$

The 3D Figure 6b, which was plotted by the RSM. The results illustrated that the a^* value was decreased as pressure increased, that is a^* value was reduced from −1.299 to −4.594 by increasing the pressure from 0.4 to 0.8 bar at the temperature of 70°C. Also, it reduced from −2.476 at a pressure of 0.4 bar to −3.128 at a pressure of 0.8 bar using a temperature of 50°C. Also, the a^* value decreased from −1.299 to −2.476 as temperature decreased from 70 to 50°C (Figure 6b). This was due to the increase of browning reaction in the milk at higher temperatures, which negatively affected the milk color, that is, an increase in a^* value.

3.3.3 | Yellowness-blueness

The results in Table 3 illustrated that the value of b^* ranged from 7.06, at 0.40 bar and 70°C to 11.53 at 0.80 bar and 70°C. The positive values of b^* indicate that the yellowness of milk color is correlated with the presence of color of carotene pigment in the milk fat. These findings agree with data reported by Gaze et al. (2015) who noticed that the b^* the value of a concentrated milk sample ranged from 17.89 ± 0.10 to 27.05 ± 0.05.

The b^* value was significantly (p <.05) affected by the Quadratic Model (QM), interfere and squared pressure (Table 4), while b^* value did not affect significantly (p > .05) by the pressure, temperature, squared pressure, and squared temperature. Besides, there was no significant (p > .05) effect for Lack of Fit. The statistical terms such as R-Squared was 0.7496, Adj. R-Squared was 0.5707, and Adequate Precision was 6.787, and standard deviation was 0.80. These statistical indicators showed that applying the QM for predicting the value of b^* as illustrated in Equation 21 can be:

$$b* = +1.40994 - 71.27174P + 0.49815T + 0.58824PT + 32.75913P^2 - 6.89635E - 003T^2 \quad (21)$$

As for the interference between temperature and pressure as depicted in Figure 6c is the 3D figure that was plotted by using RSM. The results showed that the highest value of b^* was 11.70 using 0.80 bar pressure and 70°C temperature. It was also seen that, at a pressure of 0.4 bar, the value of b^* decreased from 9.754 to 7.691 with the increase of temperature from 50 to 70°C. This observation is due to reduced Millard reactions at lower concentration temperatures (Kareb et al., 2016). It was also revealed that b^* value increased as temperature and pressure increased (Figure 6c).

3.3.4 | Chroma

The results depicted that the color density (ΔC) ranged from 4.01 at temperature of 60°C and 0.60 bar pressure to 9.01 at 0.4 bar pressure and 70°C temperature as given in Table 3. Our results disagree with data reported by Ávila et al. (2017) who observed Chroma values of 16.41.

ANOVA for Response Surface RCM illustrated that the RCM, pressure, temperature–pressure interactions, squared pressure and the interference between pressure and squared temperature have a significant (p < .05) effect on the ΔC (Table 4). Moreover, there was an insignificant (p > .05) effect of Lack of Fit as presented in Table 3. In addition, R-Squared was 0.9787, Adjusted R-Squared was 0.9490, adequate Precision was 22.521 and standard deviation was 0.28. These indicators showed that RCM can be used for predicting color intensity (ΔC) as shown in Equation 22:

$$\Delta C = +247.61327 - 367.44453P - 8.83854T + 14.25804PT - 36.06172P^2 + 0.077293T^2 + 0.23559P^2T - 0.12645PT^2 \quad (22)$$

It can be seen from Figure 6d, which was plotted by the RSM, the higher value of ΔC reached 8.92 using a pressure of 0.4 bar and temperature of 70°C compared with the pressure of 0.8 and temperature of 70°C, which was 3.92. The change in ΔC with pressure at 70°C was higher than 50°C. The interaction between pressure and temperature had a significant effect on the intensity of color where increasing pressure and decreasing temperature at the same time increased the color intensity (Figure 6e). Generally, ΔC was decreased as pressure increased at various temperatures. Log Chroma of milk reached to 1, 1.1, and 1.35 at temperatures of 70, 80, and 90°C, respectively (Güneşer, 2016).

3.3.5 | Hue angle

The results of the present investigation showed that at a concentration of temperature of 70°C, the angle of color (h) ranged between −1.37 and −1.18 rad when pressure ranged from 0.40 to 0.80 bar (Table 3). Our outcomes disagree with those reported by Ávila et al. (2017) who observed h the value of 96.47 degrees (1.68 rad).

ANOVA for Response Surface Quadratic Model (QM) showed that insignificant (p > .05) effect of QM, pressure and temperature, and the interactions between them on h. Furthermore, the Lack of Fit was significant (Table 4). The statistical parameters that were R-Squared was 0.4972, Adjusted R-Squared was 0.1380, adequate precision was 3.953 and Standard deviation was 0.63 and these parameters showed that the QM (Equation 23) cannot be used for predicting the hue angle (h):

$$h = -7.89755 - 367.44453P - 8.83854T + 14.25804PT - 36.06172P^2 + 0.07729T^2 + 0.23559P^2T - 0.12645PT^2 \quad (23)$$

The interaction between pressure and temperature values is presented as three-dimensional graphs in Figure 6e. According to the data, the highest hue angle value was 1.06 rad at 0.80 bar pressure and 60°C temperature, while the lowest was −1.413 rad using 0.60 bar pressure and 70°C temperature. Also, the results showed

that h was increased as the pressure increased and temperature decreased, that is at temperature of 70°C and 0.4 bar pressure, the h reached −1.52 rad, and increased to −0.62 rad at 0.8 bar pressure and 50°C temperature. Güneşer (2016) stated that h value was −10, −10, and 90 degrees (−0.174, −0.174, and 1.57 rad) at temperature of 70, 80, and 90°C, respectively.

3.3.6 | Browning index (BI)

According to the result of the milk concentration in Table 3, the lowest value of BI was 8.12 at pressure and temperature of 0.4 bar and 70°C, respectively. The highest value of BI was 13.58 at pressure and temperature of 0.8 bar and 60°C, respectively.

ANOVA for Response Surface RCM showed that the RCM, temperature, pressure all their interactions, and the Lack of Fit had no significant ($p > .05$) effect on the BI (Table 4). The statistical parameters were R-Squared which was 0.6817, adjusted R-Squared was 0.2360 and adequate Precision was 4.366 and Std. Dev. was 1.38, and these parameters showed that the RCM (Equation 24) cannot be used for predicting the BI due to insignificant ($p > .05$) effect of the Lack of Fit:

$$\mathrm{BI} = 57.35422 - 192.5819P - 0.87668T + 4.20226\mathrm{PT} + 52.162P^2 + 4.99216E - 003T^2 - 0.030668PT^2 - 0.069653TP^2 \quad (24)$$

As for the interaction between pressure and temperature as shown in the three-dimensional Figure 6f that was depicted by the response surface methodology, the higher BI was 12.82 at 0.80 bar pressure and 50°C temperature, while the lowest value was 8.53 using 0.40 bar pressure and 70°C temperature. Also, the results showed that BI decreased with the increase of pressure from 0.4 to 0.6, and then increased at all the studied concentration temperatures. When the temperature increased from 50 to 70°C, the BI increased from 4.89 to 11.75 at pressure of 0.8 bar. The BI is expected to be increased with increasing heating time and temperature mainly due to non-enzymatic browning reactions.

3.4 | Optimization of process

Table 5 illustrates the optimization process results of the color parameters. The results indicated that the optimum conditions of milk concentration using RW was 66°C temperature and 0.45 bar pressure. The concentrated milk at these conditions had a higher L^* (74.98) and b^* (8.27), productivity (2.25 L/h), mass of evaporated water (1.75 kg) as well as lower a^* (−2.82), ΔC (7.05), h (−1.30 rad), BI (8.88) and total heating energy (1.28 kJ). Also the results depicted that there were no significant differences between the predicted and measured data.

3.5 | Effect of the concentration method on thermos-physical attributes and color values

Table 5 shows the impact of the concentration method on the thermo-physical attributes and color parameters. The productivity of RW was higher than CC, that is, 2.3 and 1.1 L/h, respectively. Moreover, total heating energy for RW (1.28 kJ) was lower than CC (1.55 kJ).

Besides, results revealed that the concentration method had a significant effect ($p < .05$) on the L^* value. RW and CC gave a product with L^* values of 74.98 and 72.25, respectively. Also the a^* value for raw milk was −4.47, which was lower than those of RW and CC, that is a^* value for the products of RW and CC were −2.26 and −3.75, respectively.

TABLE 5 Results of the optimization process of dependent variables (practical and predicted), conventional concentration, raw milk and optimum conditions for process of milk concentration

Optimum conditions						
Pressure (bar)	Temperature (°C)	Dependent variables	Experimental	Predicted	CC	RM
0.45	66	Productivity (L/h)	2.31 ± 0.02^a	2.25 ± 0.019^a	1.10 ± 0.12^b	N/A
		Total heating energy (kJ)	1.19 ± 0.11^a	1.28 ± 0.21^a	1.55 ± 0.02^b	N/A
		Mass of evaporated water (kg)	1.77 ± 0.32^a	1.75 ± 0.14^a	0.82 ± 0.02^b	N/A
		LMTD	15.08 ± 0.13^a	15.66 ± 0.13^a	16.83 ± 0.32^b	N/A
		L^*	74.88 ± 1.38^a	74.98 ± 1.31^a	72.25 ± 1.38^b	90.98 ± 1.23^c
		a^*	-2.26 ± 1.29^a	-2.82 ± 1.24^a	-3.75 ± 1.29^b	-4.47 ± 1.01^c
		b^*	8.78 ± 0.85^a	8.27 ± 0.79^a	12.71 ± 0.85^c	8.01 ± 0.87^b
		ΔC	7.12 ± 0.21^a	7.05 ± 0.13^a	6.85 ± 0.98^b	N/A
		h (rad)	-1.31 ± 0.01^a	-1.30 ± 0.03^a	-1.28 ± 0.34^c	-1.29 ± 0.01^b
		BI	8.38 ± 0.21^a	8.88 ± 0.24^a	15.12 ± 0.54^c	5.50 ± 0.24^b

Note: The similar letter in the same column refers to no significant differences at 0.05 level. The deferent letters in the columns refer to significant differences at level 0.05.

Abbreviations: CC, conventional concentration; RM, raw milk; RW, Refractance Window at 0.45 bar and temperature of 66°C.

The increase in a^* value was due to the heating pre-treatment applied before the concentration process. On the other hand, b^* the value of raw milk increased from 8.01 to 12.71 and 8.78 after the CC and RW concentration process, respectively. This observation could be related to thermal pretreatment and standardization of milk, that is adding skim milk and cream to increase total soluble solids.

Besides, ΔC was increased after milk concentration using RW and CC compared with raw milk because of the milk standardization process and heat treatment. Furthermore, ΔC of concentrated milk by RW was lower than CC because of heating by infrared radiation transmitted from hot water. The differences between RW, CC, and raw milk were significant ($p < .05$), where h value of concentrated milk by RW was higher than CC and raw milk because a^* value was lower at using RW.

According to the results in Table 5, CC-concentrated milk possesses the highest BI followed by RW-concentrated and fresh milk samples, that is, 8.38, 15.12, and 5.50, respectively. One of the main reasons for an increase in BI is thermal treatment. As an increase in the intensity of the thermal treatment led to an increase in browning reactions, higher BI was obtained after the CC process due to the overheating of milk samples, especially the parts that were located near the heating surface. On the other hand, milk was subjected to a lower and more uniform temperature profile, which limited the Maillard reactions and color changes during the concentration process. A previous study documented that BI of a milk sample increased from 8.0 to 15.3 after an ultra-high temperature sterilization process milk at 130℃, and it reached in fresh milk due to Maillard reactions (Ansari & Sahoo, 2018).

3.6 | Microbial tests of milk and alkaline phosphatase

3.6.1 | Total count bacterial

According to Table 6, *Staphylococcus aureus*, psychrophilic, and proteolytic bacteria were not detected in the RM. On the other hand, the TCP, *Escherichia coli*, lipolytic bacteria, and total yeasts and molds were 5.03, 4.81, 4.78, and 4.51 log CFU/ml, respectively. Researchers reported that the TCP in raw milk (cow milk) reached values of 1.59 log CFU/ml (Malik et al., 2018).

In the present study, the count of total microorganisms was not calculated after 3 days of storage because of the raw milk deterioration.

Samples concentrated by RW and CC were free of tested microorganisms during the storage period of 0–90 days. In RW, the milk was in the form of a thin layer during heating, and the heat transfer occurred by radiation (infrared was emitted from hot water), which has a high ability to eliminate microorganisms as it works to generate vibrations of the water molecules in the micro-organisms. This led to their heating and killing by denaturing the proteins inside the cell (Jun et al., 2003). Besides, the rise of milk temperature to 95℃ as a pre-treatment was contributed to microorganisms inactivation during both RW and CC process. Rostami et al. (2018) stated that the RW reduced log aerobic bacteria from 6.1 to 3.7 log CFU/ml. Finally, (Nindo & Tang, 2007) reported that RW produced safe food, then it reduced log microorganisms in quash pumpkin to 0.6 log CFU/ml.

TABLE 6 Microbial tests (log CFU/ml) of raw milk and concentrated milk by Refractance Window and conventional concentration during storage periods

Microorganisms	Treatments	Storage period (day)			
		0	30	60	90
TCB	RW*	ND	ND	ND	ND
	CC	ND	ND	ND	ND
	RM	5.03	–	–	–
E.coli	RW*	ND	ND	ND	ND
	CC	ND	ND	ND	ND
	RM	4.81	–	–	–
Yeasts and molds	RW*	ND	ND	ND	ND
	CC	ND	ND	ND	ND
	RM	4.51	–	–	–
Staphylococcus aureus	RW*	ND	ND	ND	ND
	CC	ND	ND	ND	ND
	RM	ND	ND	ND	ND
Psychrophilic	RW*	ND	ND	ND	ND
	CC	ND	ND	ND	ND
	RM	ND	ND	ND	ND
Lipolytic bacteria	RW*	ND	ND	ND	ND
	CC	ND	ND	ND	ND
	RM	4.78	–	–	–
Proteolytic bacteria	RW*	ND	ND	ND	ND
	CC	ND	ND	ND	ND
	RM	ND	ND	ND	ND

Abbreviations: CC, conventional concentration; ND, not detected; RM, raw milk; RW, Refractance Window (0.45 bar and 66℃); TCP,total count bacteria; –, the milk was damaged/data not available.

3.6.2 | Alkaline phosphatase

For the Alkaline phosphatase, the results in the Table 7 showed that the alkaline phosphatase test was negative for RW and CC samples, but it was positive for RM sample. This is due to the heat treatment for milk during concentration that eliminated the alkaline phosphatase.

3.6.3 | Peroxide value and acidity during the storage time

The effect of RW, CC, and storage period at 5℃ on the peroxide value and acidity are presented in Table 8. The results illustrated that the increase of the storage period led to significant ($p < .05$) increase in peroxide value and acidity. Increasing peroxide value with the

storage period can be attributed to milk fat oxidation process occurrence as well as, due to the effect of enzymes, light, and pasteurization (Amamcharla & Metzger, 2014; Kaleem et al., 2015) Moreover, Dawodu et al. (2015) stated that the rise of temperature increases the peroxide value of plant oils. As for the increase of acidity with storage period due to temperature increase, Dawodu et al. (2015) pointed out that the rise of temperature leads to decomposed chemical bonds in fat with the presence of light and moisture, which increased the acidity. Increasing temperature leads to increase ratio of free fatty acids (Adejumo et al., 2013).

3.7 | Sensory assessment

The effect of storage period on the sensory assessments of concentrated milk by RW and CC is given in Table 9. The results illustrated that the RW score was higher than CC at all storage periods and sensory attributes. that is the odor scores of RW and CC were 40 and 36, respectively. This is because the concentration temperature by RW was lower than the CC and had no homogenization in temperature distribution during the concentration of milk. Moreover, during RW the infrared radiation was emitted from hot water and transferred to the thin layer of milk (this means that the heat transfer occurred by radiation and conduction), which did not damage milk.

TABLE 7 Alkaline phosphatase in concentrated milk using Refractance Window, conventional concentration, and raw milk

Concentration method	Pressure (bar)	Temperature (℃)	Alkaline phosphate
RW	0.40	50	Negative
		60	Negative
		70	Negative
	0.60	50	Negative
		60	Negative
		70	Negative
	0.80	50	Negative
		60	Negative
		70	Negative
CC			Negative
RM			Positive

Sensory attributes were reduced as the storage period increased. For example, when the storage period increased from 0 to 90 days, the overall acceptability decreased from 10 to 7.5, respectively. This is due to the change in chemical properties with increasing storage periods such as an increase of fatty acids and peroxides as well as acidity. The general total of sensory assessment for milk concentrated by RW was higher than CC at all storage periods.

TABLE 9 The effect of storage period on the sensory assessments of concentrated milk by Refractance Window and conventional concentration

Sensory assessment	Storage period (day)	Concentration method	
		RW*	CC
Odor	0	40 ± 1.12^{aA}	36 ± 0.78^{bA}
	30	38 ± 1.21^{aB}	34 ± 0.67^{bB}
	60	$37 \pm 1.20\text{-}^{aC}$	33 ± 0.53^{bC}
	90	35 ± 1.36^{aC}	32 ± 0.57^{bC}
Texture and body	0	29 ± 0.77^{aA}	28 ± 0.58^{bA}
	30	28 ± 0.73^{aB}	27 ± 0.52^{bB}
	60	28 ± 1.22^{aB}	26 ± 1.25^{bC}
	90	27 ± 1.30^{aC}	25 ± 1.11^{bD}
Color	0	10 ± 0.66^{aA}	8 ± 0.54^{bA}
	30	10 ± 0.45^{aA}	8 ± 0.37^{bA}
	60	9 ± 0.76^{aA}	8 ± 1.20^{bA}
	90	8 ± 0.83^{aB}	8 ± 1.12^{aA}
Taste	0	10 ± 0.12^{aA}	9 ± 0.57^{bA}
	30	9 ± 0.95^{aB}	9 ± 0.57^{aA}
	60	9 ± 1.20^{aB}	8 ± 0.47^{aB}
	90	7 ± 1.22^{aC}	7 ± 0.42^{aC}
Overall acceptability	0	10 ± 1.13^{aA}	9 ± 1.21^{bA}
	30	9 ± 1.15^{aA}	9 ± 1.11^{aA}
	60	8 ± 1.51^{aB}	8 ± 1.20^{aB}
	90	7 ± 0.14^{aC}	7 ± 0.41^{aC}
Total sum	0	99 ± 0.47^{aA}	90 ± 1.34^{bA}
	30	$3.40^{aB} \pm 94$	87 ± 1.30^{bB}
	60	$4.55^{aC} \pm 92$	83 ± 2.03^{bC}
	90	$4.39^{aD} \pm 86$	80 ± 3.33^{bD}

Note: The deferent small letters refer to significant effect between RW and CC. The deferent capital letters refer to significant effect of storage periods. RW (0.45 bar and 66℃).

TABLE 8 Peroxide value and acidity of concentrated milk by Refractance Window and conventional concentration

Parameters	Concentration method	Storage period (day)			
		0	30	60	90
Peroxide value (meq/kg fat)	RW*	0.23 ± 0.03^{aA}	0.41 ± 0.02^{aB}	0.50 ± 0.03^{bC}	0.60 ± 0.02^{bD}
	CC	0.22 ± 0.01^{bA}	0.42 ± 0.02^{aB}	0.55 ± 0.05^{aC}	0.67 ± 0.09^{aD}
Acidity (%)	RW*	0.05 ± 0.01^{aA}	0.07 ± 0.01^{aB}	0.17 ± 0.01^{aC}	0.21 ± 0.01^{aD}
	CC	0.05 ± 0.01^{aA}	0.07 ± 0.01^{aB}	0.16 ± 0.01^{bC}	0.19 ± 0.01^{aD}

Note: RW* (0.45 bar and 66℃)

4 | CONCLUSIONS

The optimization of the RW process can result in a product with better qualities (e.g., color parameters, browning index). RW gave the highest productivity and mass of evaporated water compared with CC. Moreover, total heating energy using RW was lower than CC. The score of sensory assessment of concentrated milk using RW was higher than CC. Microorganisms were eliminated completely using RW or CC. The optimum conditions were 0.45 bar pressure and 66 °C temperature. The food plants may benefit from this technology in the future after further expansion studies.

ACKNOWLEDGMENT

We would like to thank the university of Basrah for providing the food engineering laboratory and facilities.

Nomenclature

A	Sodium thiosulfate (mm)
a^*	Redness-greenness
a_0^*	Redness-greenness of raw milk
b^*	Yellowness-blueness
b_0^*	Yellowness/blueness of raw milk
BI	Browning index
C	Chroma
CVS	Computer vision system
CC	Conventional concentration
CIE	Commission International d'Eclairage
C	Specific heat (kJ/kg °C)
h	Hue angle (rad)
L^*	Lightness
L_0^*	Lightness of raw milk
L_h	Latent heat of water vaporization (kJ kg).
LMTD	Logarithm mean temperature difference (°C)
mp	Milk mass flow rate (kg/s)
M_w	Mass (kg)
Q	Total heating energy (kJ)
R	Coefficient of correlation
RCM	Reduced cubic model
RM	Raw milk
RMSE	Root mean square error
RSM	Response surface methodology
RW	Refractance Window
P	Pressure (bar)
prod.	Productivity of concentrated milk (L/h)
PN	Peroxide number
SS	Sum of squares
Std. Dev.	Standard deviation
T	Temperature (°C)
TSS	Total soluble solid (%)
W	Weight (kg)
x	Value
v	Volume (m^3)

Greek symbols

α	Coefficient
Δ	Differences

Subscripts

c	Constant pressure
μ	Cold milk temperature (°C)
θ	Cold water temperature (°C)
$\mathcal{T}$	Hot water temperature (°C)
δ	Hot milk temperature (°C)
Exp.	Experimental
°	Intercept
i	Initial
in	Inlet
f	Final
pre.	Predicted
m	Concentrated milk
out	Outlet
w	Evaporated water
1	With sample
1	Linear of pressure
11	Quadratic of P^2
2	Linear of temperature
2	Without sample
12	P × T (interaction terms)
22	Quadratic of T^2

CONFLICTS OF INTEREST

The authors have declared no conflicts of interest for this article.

AUTHOR CONTRIBUTIONS

Conceptualization; Data curation; Formal analysis; Funding acquisition; Investigation; Methodology; Project administration; Resources; Software; Supervision; Visualization; Writing-original draft; Writing-review & editing: Asaad Al-Hilphy. *Conceptualization; Data curation; Investigation; Writing-original draft*: Haider I Ali. *Data curation; Investigation; Methodology; Writing-original draft*: Sajedah A. Al-IEssa. *Writing-review & editing*: Jose Manuel Lorenzo. *Writing-review & editing*: Francisco Jose J Barba. *Methodology; Supervision; Visualization; Writing-review & editing*: Mohsen Gavahian.

DATA AVAILABILITY STATEMENT

Data available on request from the authors.

ORCID

Asaad R. Al-Hilphy https://orcid.org/0000-0001-5850-1519
José M. Lorenzo https://orcid.org/0000-0002-7725-9294
Francisco J. Barba https://orcid.org/0000-0002-5630-3989
Mohsen Gavahian https://orcid.org/0000-0002-4904-0519

REFERENCES

A.O.A.C. (2016). *Official methods of analysis of AOAC international*. AOAC International. ISBN 978-0-935584-87-5.

Abonyi, B. I., Feng, H., Tang, J., Edwards, C. G., Mattinson, D. S., & Fellman, J. K. (2002). Quality retention in strawberry and carrot purees dried with Refractance Window® system. *Journal of Food Science*, *67*, 1051–1056. https://doi.org/10.1111/j.1365-2621.2002.tb09452.x

Adejumo, B. A., Alakowe, A. T., & Obi, D. E. (2013). Effect of heat treatment on the characteristics and oil yield of *Moringa oleifera* seeds. *International Journal of Engineering Science*, *2*, 232–239.

Al-Hilphy, A. R. S., Ali, H. I., & Mohsin, G. F. (2019). Technology of Ohmic heating for the pasteurization of milk for the pasteurization of milk. In M. R. Goyal, & A. K. Gupta (Eds.), *Novel Dairy Processing Technologies* (1st ed., pp. 3–46). Apple Academic Press. https://doi.org/10.1201/9781315167121-1

Al-Hilphy, A. R., Ali, H. I., Al-IEssa, S. A., Lorenzo, J. M., Barba, F. J., & Gavahian, M. (2020). Optimization of process variables on physicochemical properties of milk during an innovative refractance window concentration. *Journal of Food Processing and Preservation*, *44*, e14782. https://doi.org/10.1111/jfpp.14782

Amamcharla, J. K., & Metzger, L. E. (2014). Modification of the ferric reducing antioxidant power (FRAP) assay to determine the susceptibility of raw milk to oxidation. *International Dairy Journal*, *34*, 177–179. https://doi.org/10.1016/j.idairyj.2013.09.004

Ansari, I. A., & Sahoo, P. K. (2018). Color variation of ultra high temperature (UHT) sterilized milk during storage. *International Journal of Chemical Studies*, *6*, 754–757.

Ávila, M., Gómez-Torres, N., Delgado, D., Gaya, P., & Garde, S. (2017). Effect of high-pressure treatments on proteolysis, volatile compounds, texture, colour, and sensory characteristics of semi-hard raw ewe milk cheese. *Food Research International*, *100*, 595–602. https://doi.org/10.1016/j.foodres.2017.07.043

Bernaert, N., Van Droogenbroeck, B., Van Pamel, E., & De Ruyck, H. (2019). Innovative refractance window drying technology to keep nutrient value during processing. *Trends in Food Science & Technology*, *84*, 22–24. https://doi.org/10.1016/j.tifs.2018.07.029

Belfield, A., & Goldberg, D. (1971). Colorimetric determination of alkaline phosphatase activity. *Enzyme*, *12*(5), 561–568. https://doi.org/10.1016/j.tifs.2018.07.029

Clark, S., Costello, M., Drake, M., & Bodyfelt, F. (2009). *The sensory evaluation of dairy products*. Springer. https://doi.org/10.1016/j.jfoodeng.2014.03.029

da Silva, W. P., Hamawand, I., & e Silva, C. M. D. P. S. (2014). A liquid diffusion model to describe drying of whole bananas using boundary-fitted coordinates. *Journal of Food Engineering*, *137*, 32–38. https://doi.org/10.1016/j.jfoodeng.2014.03.029

Darvishi, H., Hosainpour, A., Nargesi, F., & Fadavi, A. (2015). Exergy and energy analyses of liquid food in an Ohmic heating process: A case study of tomato production. *Innovative Food Science & Emerging Technologies*, *31*, 73–82. https://doi.org/10.1016/j.ifset.2015.06.012

Dawodu, M. O., Olutona, G. O., & Obimakinde, S. O. (2015). Effect of temperature on the chemical characteristics of vegetable oils consumed in Ibadan, Nigeria. *Pakistan Journal of Nutrition*, *14*, 698. https://doi.org/10.3923/pjn.2015.698.707

Faion, A. M., Becker, J., Fernandes, I. A., Steffens, J., & Valduga, E. (2019). Sheep's milk concentration by ultrafiltration and cheese elaboration. *Journal of Food Process Engineering*, *42*(4), e13058. https://doi.org/10.1111/jfpe.13058

Fernández-Vázquez, R., Stinco, C. M., Hernanz Vila, D., Heredia, F. J., Chaya, C., & Vicario, I. M. (2018). Internal preference mapping of milk-fruit beverages: Influence of color and appearance on its acceptability. *Food Sciences and Nutrition*, *6*, 27–35. https://doi.org/10.1002/fsn3.494

Gaze, L. V., Costa, M. P., Monteiro, M. L. G., Lavorato, J. A. A., Conte Júnior, C. A., Raices, R. S. L., Cruz, A. G., & Freitas, M. Q. (2015). Dulce de Leche, a typical product of Latin America: Characterisation by physicochemical, optical and instrumental methods. *Food Chemistry*, *169*, 471–477. https://doi.org/10.1016/j.foodchem.2014.08.017

Güneşer, O. (2016). Pigment and color stability of beetroot betalains in cow milk during thermal treatment. *Food Chemistry*, *196*, 220–227. https://doi.org/10.1016/j.foodchem.2015.09.033

Hadimani, L., & Mittal, N. (2019). Development of a computer vision system to estimate the colour indices of Kinnow mandarins. *Journal of Food Science and Technology*, *56*, 2305–2311. https://doi.org/10.1007/s13197-019-03641-9

Harrigan, W. F., & McCance, M. E. (1976). *Laboratory methods in food and dairy microbiology*. Academic Press Inc. (London) Ltd.

Jun, S., Irudayaraj, J., Demirci, A., & Geiser, D. (2003). Pulsed UV-light treatment of corn meal for inactivation of *Aspergillus niger* spores. *International Journal of Food Science & Technology*, *38*, 883–888. https://doi.org/10.1046/j.0950-5423.2003.00752.x

Kaleem, A., Aziz, S., & Iqtedar, M. (2015). Investigating changes and effect of peroxide values in cooking oils subject to light and heat. *FUUAST Journal of Biology*, *5*, 191–196.

Kareb, O., Champagne, C. P., & Aïder, M. (2016). Contribution to the production of lactulose-rich whey by in situ electro-isomerization of lactose and effect on whey proteins after electro-activation as confirmed by matrix-assisted laser desorption/ionization time-of-flight-mass spectrometry and sodium. *Journal of Dairy Science*, *99*, 2552–2570. https://doi.org/10.3168/jds.2015-10037

Keyser, M., Műller, I. A., Cilliers, F. P., Nel, W., & Gouws, P. A. (2008). Ultraviolet radiation as a non-thermal treatment for the inactivation of microorganisms in fruit juice. *Innovative Food Science & Emerging Technologies*, *9*(3), 348–354.

Khuri, A. I., & Cornell, J. A. (2019). *Response surfaces: Designs and analyses* (2nd ed.). CRC Press. https://doi.org/10.1201/9780203740774

Konovalov, V. I., Gatapova, N. Z., Koliuch, A. N., Pachomov, A. N., Shikunov, A. N., & Utrobin, A. N. (2004). Kinetics of conductive drying and heat-transfer on contact cylinders. In *Proceedings of the 14th International Drying Symposium*, 247–253).

Lei, T., & Sun, D.-W. (2019). Developments of nondestructive techniques for evaluating quality attributes of cheeses: A review. *Trends in Food Science & Technology*, *88*, 527–542. https://doi.org/10.1016/j.tifs.2019.04.013

Malik, N. S., Lani, M. N., & Ahmad, F. T. (2018). Stability of lactic acid bacteria and physico-chemical properties of pasteurized cow's and goat's milk. *Malaysian Journal of Fundamental and Applied Sciences*, *ICAFT2018*, 341–345). https://doi.org/10.11113/mjfas.v15n2-1.1560

McDermott, A., Visentin, G., McParland, S., Berry, D. P., Fenelon, M. A., & De Marchi, M. (2016). Effectiveness of mid-infrared spectroscopy to predict the color of bovine milk and the relationship between milk color and traditional milk quality traits. *Journal of Dairy Science*, *99*, 3267–3273. https://doi.org/10.3168/jds.2015-10424

Minz, P. S., & Saini, C. S. (2019). Evaluation of RGB cube calibration framework and effect of calibration charts on color measurement of mozzarella cheese. *Journal of Food Measurement and Characterization*, *13*, 1537–1546. https://doi.org/10.1007/s11694-019-00069-9

Misawa, N., Barbano, D. M., & Drake, M. A. (2016). Influence of casein as a percentage of true protein and protein level on color and texture of milks containing 1 and 2% fat. *Journal of Dairy Science*, *99*, 5284–5304. https://doi.org/10.3168/jds.2016-10846

Moejes, S. N., van Wonderen, G. J., Bitter, J. H., & van Boxtel, A. J. B. (2020). Assessment of air gap membrane distillation for milk concentration. *Journal of Membrane Science*, *594*, 117403. https://doi.org/10.1016/j.memsci.2019.117403

Morison, K. R., Worth, Q. A. G., & O'dea, N. P. (2006). Minimum wetting and distribution rates in falling film evaporators. *Food and Bioproducts Processing*, *84*, 302–310. https://doi.org/10.1205/fbp06031

Nindo, C. I., & Tang, J. (2007). Refractance window dehydration technology: A novel contact drying method. *Drying Technology*, *25*, 37–48. https://doi.org/10.1080/07373930601152673

Owens, S. L., Brewer, J. L., & Rankin, S. A. (2001). Influence of bacterial cell population and pH on the color of nonfat milk. *LWT–Food*

Science and Technology, *34*(5), 329–333. https://doi.org/10.1006/fstl.2001.0781

Palou, E., López-Malo, A., Barbosa-Cánovas, G. V., Welti-Chanes, J., & Swanson, B. G. (1999). Polyphenoloxidase activity and color of blanched and high hydrostatic pressure treated banana puree. *Journal of Food Science*, *64*, 42–45. https://doi.org/10.1111/j.1365-2621.1999.tb09857.x

Paramalingam, S., Winchester, J., & Marsh, C. (2000). On the fouling of falling film evaporators due to film break-up. *Food and Bioproducts Processing*, *78*, 79–84. https://doi.org/10.1205/096030800532770

Parmar, P., Singh, A. K., Meena, G. S., Borad, S., & Raju, P. N. (2018). Application of ohmic heating for concentration of milk. *Journal of Food Science and Technology*, *55*, 4956–4963. https://doi.org/10.1007/s13197-018-3431-4

Pehlivan, H., & Özdemir, M. (2012). Experimental and theoretical investigations of falling film evaporation. *Heat and Mass Transfer*, *48*, 1071–1079. https://doi.org/10.1007/s00231-011-0962-x

Raghavi, L. M., Moses, J. A., & Anandharamakrishnan, C. (2018). Refractance window drying of foods: A review. *Journal of Food Engineering*, *222*, 267–275. https://doi.org/10.1016/j.jfoodeng.2017.11.032

Rossi, G., Schiavon, S., Lomolino, G., Cipolat-Gotet, C., Simonetto, A., Bittante, G., & Tagliapietra, F. (2018). Garlic (*Allium sativum* L.) fed to dairy cows does not modify the cheese-making properties of milk but affects the color, texture, and flavor of ripened cheese. *Journal of Dairy Science*, *101*, 2005–2015. https://doi.org/10.3168/jds.2017-13884

Rostami, H., Dehnad, D., Jafari, S. M., & Tavakoli, H. R. (2018). Evaluation of physical, rheological, microbial, and organoleptic properties of meat powder produced by Refractance Window drying. *Drying Technology*, *36*(9), 1076–1085. https://doi.org/10.1080/07373937.2017.1377224

Scarso, S., McParland, S., Visentin, G., Berry, D. P., McDermott, A., & De Marchi, M. (2017). Genetic and nongenetic factors associated with milk color in dairy cows. *Journal of Dairy Science*, *100*, 7345–7361. https://doi.org/10.3168/jds.2016-11683

Silveira, A. C. P., de Carvalho, A. F., Perrone, Í. T., Fromont, L., Méjean, S., Tanguy, G., Jeantet, R., & Schuck, P. (2013). Pilot-scale investigation of effectiveness of evaporation of skim milk compared to water. *Dairy Science & Technology*, *93*, 537–549. https://doi.org/10.1007/s13594-013-0138-1

Silveira, A. C. P., Tanguy, G., Perrone, Í. T., Jeantet, R., Ducept, F., de Carvalho, A. F., & Schuck, P. (2015). Flow regime assessment in falling film evaporators using residence time distribution functions. *Journal of Food Engineering*, *160*, 65–76. https://doi.org/10.1016/j.jfoodeng.2015.03.016

Taheri-Garavand, A., Fatahi, S., Omid, M., & Makino, Y. (2019). Meat quality evaluation based on computer vision technique: A review. *Meat Science*, *156*, 183–195. https://doi.org/10.1016/j.meatsci.2019.06.002

Tanguy, G., Tuler-Perrone, I., Dolivet, A., Santellani, A.-C., Leduc, A., Jeantet, R., Schuck, P., & Gaucheron, F. (2019). Calcium citrate insolubilization drives the fouling of falling film evaporators during the concentration of hydrochloric acid whey. *Food Research International*, *116*, 175–183. https://doi.org/10.1016/j.foodres.2018.08.009

Tomasević, I., Tomović, V., Milovanović, B., Lorenzo, J., Đorđević, V., Karabasil, N., & Đekić, I. (2019). Comparison of a computer vision system vs. traditional colorimeter for color evaluation of meat products with various physical properties. *Meat Science*, *148*, 5–12. https://doi.org/10.1016/j.meatsci.2018.09.015

Wasnik, P. G., Menon, R. R., Sivaram, M., Nath, B. S., Balasubramanyam, B. V., & Manjunatha, M. (2019). Development of mathematical model for prediction of adulteration levels of cow ghee with vegetable fat using image analysis. *Journal of Food Science and Technology*, *56*, 2320–2325. https://doi.org/10.1007/s13197-019-03677-x

Yam, K. L., & Papadakis, S. E. (2004). A simple digital imaging method for measuring and analyzing color of food surfaces. *Journal of Food Engineering*, *61*, 137–142. https://doi.org/10.1016/S0260-8774(03)00195-X

Yanniotis, S. (2007). *Solving problems in food engineering* (302 pp.). Springer Science and Business Media. https://doi.org/10.1007/978-0-387-73514-6

Zotarelli, M. F., Carciofi, B. A. M., & Laurindo, J. B. (2015). Effect of process variables on the drying rate of mango pulp by Refractance Window. *Food Research International*, *69*, 410–417. https://doi.org/10.1016/j.foodres.2015.01.013

How to cite this article: Al-Hilphy, A. R., Ali, H. I., Al-IEssa, S. A., Lorenzo, J. M., Barba, F. J., & Gavahian, M. (2021). Refractance window (RW) concentration of milk-Part II: Computer vision approach for optimizing microbial and sensory qualities. *Journal of Food Processing and Preservation*, 00, e15702. https://doi.org/10.1111/jfpp.15702